RESEARCH ARTICLE

Cyanidin-3-glucoside and its phenolic acid metabolites attenuate visible light-induced retinal degeneration in vivo via activation of Nrf2/HO-1 pathway and NF-κB suppression

*Yong Wang, Yazhen Huo, Liang Zhao, Feng Lu, Ou Wang, Xue Yang, Baoping Ji and Feng Zhou**

Beijing Key Laboratory of Functional Food from Plant Resources, College of Food Science & Nutritional Engineering, China Agricultural University, Beijing, People's Republic of China

Received: December 19, 2015
Revised: February 23, 2016
Accepted: February 24, 2016

Scope: Cyanidin-3-glucoside (C3G) is a major anthocyanin in berries and a potential nutritional supplement for preventing retinal degeneration. However, the protective mechanism of C3G and its metabolites, protocatechuic acid (PCA) and ferulic acid (FA), remain unclear. The molecular mechanisms of C3G and its metabolites against retinal photooxidative damage in vivo are investigated.

Methods and results: Pigmented rabbits were orally administered C3G, PCA, and FA (0.11 mmol/kg/day) for 3 weeks. Electroretinography, histological analysis, and TUNEL assay showed that C3G and its metabolites attenuated retinal cell apoptosis. The expression of oxidative stress markers were upregulated after light exposure but attenuated by C3G and FA, which may be attributed to the elevated secretion and expression of heme oxygenase (HO-1) and nuclear factor erythroid-2 related factor 2 (Nrf2). C3G, PCA, and FA attenuated the secretion or expression of inflammation-related genes; FA suppressed nuclear factor kappa B (NF-κB) activation. The treatments attenuated the light-induced changes on certain apoptotic proteins and angiogenesis-related cytokines.

Conclusion: C3G and FA reduced light-induced retinal oxidative stress by activating the Nrf2/HO-1 antioxidant pathway. FA attenuated the light-induced retinal inflammation by suppressing NF-κB activation. C3G and its metabolites attenuated the photooxidation-induced apoptosis and angiogenesis in the retina.

Keywords:
Cyanidin-3-glucoside / Phenolic acid metabolites / Oxidative stress / Inflammation / Retinoprotection

1 Introduction

Exposure to excessive visible light can induce retinal oxidative stress and inflammation, which leads to the onset and/or progression of retinal degeneration [1, 2]. The retina is the most metabolically active tissue in the body; its high oxygen tension, high levels of light exposure, and high concentration of polyunsaturated fatty acids (PUFAs) cause photoreceptors to be particularly susceptible to light damage [3,4]. Age-related macular degeneration (AMD) is the most common cause of irreversible vision loss in the elderly worldwide [4]. Although

Correspondence: Baoping Ji
E-mail: jbp330332@gmail.com

Abbreviations: 8-OHdG, 8-hydroxydeoxyguanosine; **ACN**, anthocyanin; **AMD**, age-related macular degeneration; **C3G**, cyanidin-3-glucoside; **COX-2**, cyclooxygenase 2; **ERG**, electroretinogram; **FA**, ferulic acid; **GCL**, ganglion cell layer; **HE**, hematoxylin and eosin; **HIF-1α**, hypoxia-inducible factor-1α; **HNE**, 4-hydroxynonenal; **HO-1**, heme oxygenase-1; **IL-1β**, interleukin-1 β; **IL-8**, interleukine-8; **INL**, inner nuclear layer; **MAPK**, mitogen-activated protein kinase; **MCP-1**, monocyte chemoattractant protein 1; **NF-κB**, nuclear factor kappa B; **Nrf2**, nuclear factor erythroid-2 related factor 2; **ONH**, optic nerve head; **ONL**, outer nuclear layer; **PCA**, protocatechuic acid; **PUFAs**, polyunsaturated fatty acids; **RPE**, retinal pigment epithelial; **TNF-α**, tumor necrosis factor-alpha; **VEGF**, vascular endothelial growth factor

Colour online: See the article online to view Figs. 3, 4, and 10 in colour.

*Additional corresponding author: Feng Zhou,
E-mail: bjwfyz_zf@163.com

© 2016 WILEY-VCH Verlag GmbH & Co. KGaA, Weinheim

the pathogenesis of AMD is not fully understood, increasing evidence suggests that oxidative stress and inflammation may play important roles [2].

Anthocyanins (ACNs) are beneficial for vision because they promote the reproduction of rhodopsin, increase the circulation within the retinal capillaries, improve impaired night vision, and decrease macular degeneration and diabetic retinopathy [5–7]. The most abundant ACN in the edible parts of plants is cyanidin-3-glucoside (C3G) [8]. C3G facilitates rhodopsin regeneration in rod photoreceptors, interacts directly with the dark and light forms of rhodopsin and opsin protein, and inhibits the photooxidation of retinal pigment epithelial (RPE) cells [9–13]. In addition, C3G can be detected in the eyes by oral administration of blueberry, thereby suggesting its possible role in protecting against retinal diseases [14]. However, the underlying mechanism of C3G against light-induced retinal degeneration is still unclear. To our knowledge, limited information is available on the effect of pure C3G on retinal protection in vivo, especially the visible light-induced retinal degeneration.

A previous study showed that 69% of the ACNs disappeared from the gastrointestinal tract within 4 h after food ingestion [15]. A human study suggested that part of this disappearance can be attributed to the degradation of ACN aglycones, thereby leading to the formation of the corresponding phenolic acids [15]. In particular, protocatechuic acid (PCA) and ferulic acid (FA) are the major human metabolites of C3G in plasma after C3G consumption [16]. High concentrations of PCA and FA may explain the short-term increase in plasma and retina antioxidant activity observed after eating C3G-rich food, which can also contribute to visual health.

Epidemiological studies suggest that dietary ACNs attenuate retinal degeneration [17]. However, given the biological instability and extensive metabolism of ACNs [16], their degradation products, especially phenolic acids, are probably responsible for retina protective bioactivity. Phenolic acids have shown beneficial effects on retinal degeneration in vitro and in vivo [18–20]. Chlorogenic acid is responsible for reduction of the apoptosis of retinal cells induced by hypoxia and NO [18]. Chicoric acid can ameliorate the oxidative stress-induced degeneration of retinal ganglion cells through its antioxidative and antiapoptotic effects [19]. Hydrocaffeic acid protects against ocular inflammation and cell oxidation damage induced by UV-B in vivo [20]. However, whether C3G or the metabolites of C3G (PCA and FA) are more effective in protecting the retina from light-induced degeneration has yet to be elucidated.

In the present study, we investigated C3G and its major metabolites PCA and FA (Fig. 1) for the first time in an in vivo model of visible light-induced retinal degeneration and demonstrated the related molecular mechanisms. Retinal function and the histological integrity of the retina were investigated to compare the protective effects of C3G, PCA, and FA in this model. This model in pigmented rabbits has been used to evaluate the retinoprotective effects of molecules in retinal degeneration, because of its similar mechanisms to human retinal degeneration, such as oxidative stress, inflammation, apoptosis, and angiogenesis [21]. This study provides insights into the confirmation of authentic molecules that protect against light damage when consuming C3G-rich diets.

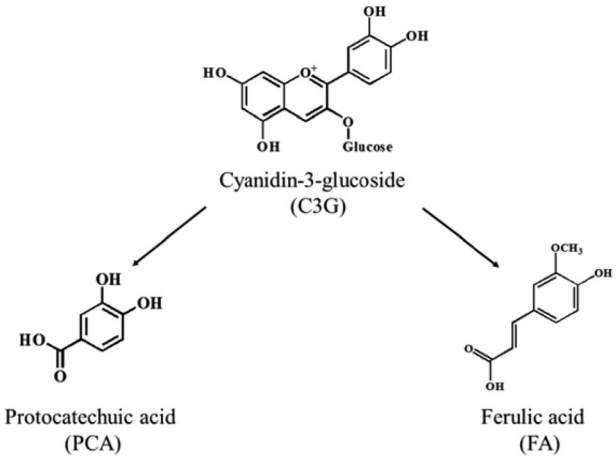

Figure 1. Chemical structures of C3G, PCA, and FA.

2 Materials and methods

2.1 Chemicals

C3G (98.4%), PCA (99.9%), and FA (98.8%) were purchased from Nanjing Jingzhu Bio-technology, Ltd. (Nanjing, Jiangsu, China). Tropicamide eye drops were purchased from Xingqi Pharmaceuticals Co., Ltd. (Shenyang, China). Sumianxin was purchased from Shengda Pharmaceuticals Co., Ltd. (Dunhua, China). Anti-caspase-3, anti-Ho-1, anti-NF-κB, anti-caspase-9, and anti-VEGF were purchased from Abcam (Cambridge, UK). Anti-Bcl-2 was purchased from Abnova (Taipei, Taiwan). Anti-Bax was purchased from Enzo Life Sciences (New York, NY, USA). Anti-β-actin was purchased from Cell Signaling Technology (Danvers, MA, USA). The radioimmunoprecipitation assay (RIPA) buffer and bicinchoninic acid (BCA) protein assay kit were purchased from Beyotime Institute of Biotechnology (Shanghai, China). The nuclear factor erythroid-2 related factor 2 (Nrf2), 4-hydroxynonenal (HNE), 3-nitrotyrosine, 8-hydroxydeoxyguanosine (8-OHdG), monocyte chemoattractant protein 1 (MCP-1), interleukin-8 (IL-8), interleukin-1 β (IL-1β), tumor necrosis factor-alpha (TNF-α), cyclooxygenase 2 (COX-2), and hypoxia-inducible factor-1α (HIF-1α) assay kits were purchased from Keyingmei Biotechnology and Science, Inc. (Beijing, China). All other chemicals and reagents were purchased from Sigma-Aldrich (St. Louis, MO, USA).

2.2 Animal care

A total of 40 healthy pigmented rabbits weighing 2.5–3.0 kg were purchased from the Animal Center of Beijing Kaiyuan

© 2016 WILEY-VCH Verlag GmbH & Co. KGaA, Weinheim

Co. (Beijing, China). All procedures were performed in accordance with the Association for Research in Vision and Ophthalmology Statement for Use of Animals in Ophthalmic and Vision Research. The procedures were approved by the Ethical Committee for Animal Experimentation of the First Hospital Affiliated to General Hospital of the Chinese People's Liberation Army (Permit number AERB20150089). All rabbits were housed at a 12 h/12 h light/dark cycle for 1 week at 22–25°C and 55–60% humidity. All rabbits were freely fed a standard maintenance diet (Beijing KEAO XIELI FEED Co., Ltd., China).

2.3 Treatment with C3G, PCA, and FA and exposure to visible light

After a week-long adaptation period, the rabbits were randomly divided into five groups ($n = 8$ per group), as follows: normal group (no light exposure and vehicle administration; NG), light-induced retinal damage model group (18 000 lx light exposure and vehicle administration; MG), the C3G group (18 000 lx light exposure and administration of C3G, 50.00 mg/kg/day), the PCA group (18 000 lx light exposure and administration of PCA, 17.15 mg/kg/day), and the FA group (18 000 lx light exposure and administration of FA, 21.61 mg/kg/day). C3G, PCA, and FA were administered at the same molar concentration for each group (0.11 mmol/kg body weight). C3G, PCA, and FA were suspended in PBS and intragastrically administered to the respective rabbits. PBS alone was intragastrically administered to the rabbits in the NG and MG groups. The rabbits were treated with C3G, PCA, and FA for 2 weeks of pre-illumination and 1 week of post-illumination until sacrifice.

The light exposure method was adopted from our previous study [21]. In brief, after dark adaptation (60–100 lx) for 24 h, the pupils were dilated with tropicamide eye drops at 20 min before light exposure. The nonanesthetized rabbits were then exposed to 18 000 ± 1000 lx of four diffused cool-white fluorescent lights for 2 h in cages with reflective interiors. The temperature during light exposure was maintained at 25 ± 1.5°C. After light exposure, the rabbits were placed in the dark for 24 h before they were returned to the normal light/dark cycle.

2.4 Electroretinographic analysis

Electroretinograms (ERGs) were recorded by a visual electrophysiology system (APS-2000AER; Kanghua Rui Ming Technology Co., Ltd., Chongqing, China) to measure retinal function at 7 days after light exposure as described in our previous study [22]. In brief, after dark adaptation for more than 1 h, the rabbits were anesthetized with an intramuscular injection of sumianxin (0.2 mL/kg) to reduce discomfort. Pupils were fully dilated with tropicamide eye drops. The ERGs were recorded in accordance with the standards set by the International Society for Clinical Electrophysiology of Vision. All procedures were performed in dim red light.

2.5 Hematoxylin and eosin (HE) staining and measurement of outer nuclear layer (ONL) thickness

Rabbits were sacrificed after the ERG recording. HE staining was performed according to the method used in our previous study [21]. Briefly, the eyeballs were quickly enucleated and immersed for 48 h in a fixative solution containing 2.5% glutaraldehyde and 2% paraformaldehyde. Samples were embedded in paraffin while considering sample orientation, and 4 μm slides were prepared with a microtome. Twelve paraffin-embedded sections were cut through the optic nerve head (ONH) of each eye and stained with HE. Micrographs were photographed by light microscope (Leica, Heidelberg, Germany), and the ONL thickness was counted within 250–2750 μm (counted at 500 μm intervals) of the superior and inferior edges to the ONH based on the photographs of HE-stained sections by personnel blinded to the study groups. The mean ONL thickness was calculated from 12 sections for each retina.

2.6 TUNEL analysis

TUNEL analysis was performed with an apoptosis detection kit (Roche, Mannheim, Germany) according to the manufacturer's instructions. In brief, paraffin-embedded retinal sections were deparaffinized, rehydrated, digested with protein K, and labeled with the TUNEL reaction mixture by incubation for 60 min at 37°C. For each retina, the number of TUNEL-positive cells in the inner nuclear layer (INL) and the ganglion cell layer (GCL) were counted according to our previous study [22]. Data from all fields and all retinas were pooled to obtain the apoptotic index, which is the percentage of TUNEL positive cells in the INL and GCL that were manually counted in ten randomly selected fields.

2.7 ELISA

Whole retinas were dissected and placed into lysis buffer with protease inhibitors (Roche, Mannheim, Germany), and the samples were sonicated for 10 s on ice. After centrifuging the lysates at 15 000 × *g* for 30 min at 4°C, and supernatant was collected. The concentrations of HNE, 3-nitrotyrosine, 8-OHdG, Nrf2, MCP-1, IL-8, IL-1β, and HIF-1α in retinal tissue supernatants were determined with commercial assay kits from Keyingmei Biotechnology and Science Inc. (Beijing, China). The protein concentrations were determined with the BCA protein assay kit from Beyotime Institute of Biotechnology (Shanghai, China).

© 2016 WILEY-VCH Verlag GmbH & Co. KGaA, Weinheim

Table 1. Primer sequences of genes

Gene	GenBank numbers	Product length (bp)	Primer	Primer sequence (5′-3′)
HO-1	XM_002711415	100	Forward	CAGGTGACTGCCGAGGGTT
			Reverse	GACCGGGTTCTCCTTGTTGTG
Nrf2	XM_008258230	148	Forward	CTCCATATCCCATTCCCTGTA
			Reverse	TCTGAGCAGCCACTTTATTCT
MCP-1	NM_001082294	157	Forward	CTCATAGCAGTCGCCTTCAGC
			Reverse	CAGCTTCTTTGGGACACTTGG
IL-8	NM_001082293	122	Forward	CCACACCTTTCCATCCCAAAT
			Reverse	CTTCTGCACCCACTTTTCCTTG
IL-1β	NM_001082201	142	Forward	CTTGTCAGTCGTTGTGGCTCT
			Reverse	GTAGTCATCCCAGGTGTTGCA
β-Actin	NM_001101683	177	Forward	CGTGCGGGACATCAAGGAG
			Reverse	AGGAAGGAGGGCTGGAAGAG

2.8 Western blot analysis

The retinal protein samples were collected, and the total protein concentration was determined with the BCA protein assay kit. Western blot analysis was performed as previously described [21]. In brief, equal aliquots (20–30 μg) of protein samples were applied to 10% sodium dodecyl sulfate polyacrylamide gels and electrophoretically separated. Resolved proteins were electrophoretically transferred to nitrocellulose membranes (Millipore, Bedford, MA, USA) and blocked with 5% nonfat dry milk. The membranes were incubated with HO-1 (1:500), NF-κB (1:1000), caspase-9 (1:500), Bax (1:1000), Bcl-2 (1:20), VEGF (1:500), or β-actin (1:5000) antibodies for 2 h, followed by incubation with the appropriate horseradish peroxidase-conjugated secondary antibody for 2 h. The signals were visualized by enhanced chemiluminescence (Fisher/Pierce, Rockford. IL, USA) and recorded on X-ray films (Eastman Kodak Company, Rochester, NY, USA). The intensities of the protein bands were determined with the ImageJ software (1.32j, National Institutes of Health, Bethesda, MD, USA). The band densities of each sample were normalized to the β-actin band.

2.9 Immunohistochemistry

The immunohistological staining was performed according to our previous study [21]. In brief, 4 μm sections were placed in an antigen retrieval solution (0.01 mol/L citrate buffer, pH 6.0) for 15 min in a microwave oven at 100°C and 600 W. The samples were incubated at 4°C overnight in a primary antibody solution of anti-caspase-3 (ab2171, 1:50). After washing, the samples were incubated with horseradish peroxidase-conjugated secondary antibodies (1:200, Dako, Glostrup, Denmark) for 60 min at room temperature, developed with 3,3′-diaminobenzide tetrahydrochloride, counterstained with hematoxylin, dehydrated, and mounted. The extent and intensity of immunopositivity were both considered during the scoring of caspase-3 expression. The final score, which ranged from 0 to 12, was determined by multiplying the intensity and quantity scores.

2.10 RNA extraction and quantitative real-time PCR

The total RNA was extracted with Trizol (Invitrogen, Carlsbad, CA, USA). The isolated RNA sequencing samples were used to perform real-time quantitative (qRT-PCR) analysis. First-strand cDNA was synthesized with M-MLV Reverse Transcriptase (NEB, USA). Primer Premier 5.0 (Premier Biosoft International, Palo Alto, CA, USA) was used to design the primers, which are shown Table 1. All primers listed in Table 1 were synthesized by BGI (Beijing, China). Finally, the expression of these related genes was detected by the ViiA 7 Real-Time PCR System (Applied Biosystems). The method of operation was according to the manufacturer's instructions, and the dye used was SYBR Green (Applied Biosystems, Foster City, CA, USA). The quantification of gene expression with real-time PCR data was calculated relative to β-actin. All reactions were performed in biological (three rabbits) and technical (three qPCR replicates per biological sample) triplicates. The relative expression levels were calculated by the $2^{-\Delta\Delta Ct}$ method [23].

2.11 Statistical analysis

Results were presented as mean ± standard deviation. Differences between groups were assessed by one-way ANOVA, followed by Duncan's multiple range tests. A normality test showed that all the raw data had a normal distribution, and all groups had equal variance by a variance test. Statistical significance was set at $p < 0.05$. All statistical analyses were performed with the SPSS statistical program (version 21 software, SPSS Inc. Chicago, USA).

3 Results

3.1 Functional evaluation by ERG

To determine the effects of C3G, PCA, and FA on visual function, we recorded the amplitudes of the b-wave ERGs at 7 days after light exposure. In MG rabbits, we observed significant reductions in scotopic and photopic b-wave amplitudes (35.3

© 2016 WILEY-VCH Verlag GmbH & Co. KGaA, Weinheim

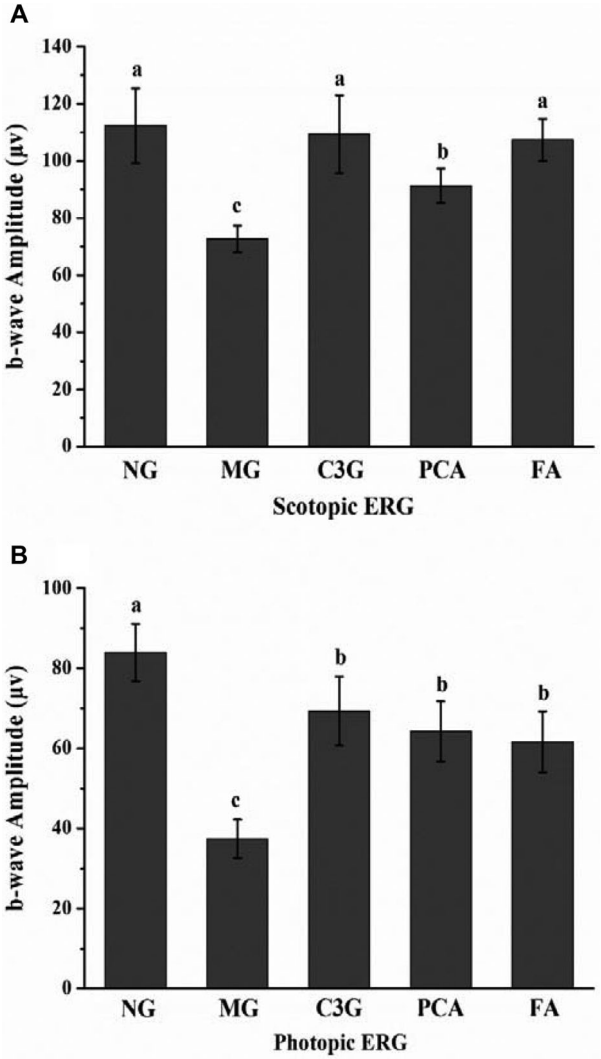

Figure 2. b-wave amplitudes of (A) scotopic ERG and (B) photopic ERG from retinas in rabbits in the NG, MG, C3G, PCA, and FA groups at 7days after light exposure. Data are expressed as the mean ± standard deviation ($n = 8$). Bars not sharing a common letter are significantly different ($p<0.05$) from each other, assayed by one-way ANOVA, followed by Duncan's multiple range test.

and 55.4%, respectively) compared to NG rabbits ($p < 0.05$; Fig. 2). After administration of C3G, PCA, and FA, the reduction in scotopic ERG b-wave amplitudes were significantly decreased by 92.5, 46.9, and 87.5%, respectively ($p < 0.05$; Fig. 2A). C3G, PCA, and FA protected against the reduction of these amplitudes of photopic ERG by 68.5, 57.6, and 52.1%, respectively ($p < 0.05$; Fig. 2B).

3.2 ONL thickness

C3G, PCA, and FA protect against light-induced loss of retinal function. Thus, we determined whether the retinal structure was also preserved by their supplementation. At 7 days after light exposure, a significant decrease in the ONL thickness was observed in retinas from MG rabbits ($p < 0.05$; Fig. 3). After administration of C3G, PCA, and FA, the thinning of the ONL was significantly reduced by 45.0, 25.5, and 46.6, respectively ($p < 0.05$), which implied that these treatments protected the photoreceptor cells from light-induced damage.

3.3 Retinal cell apoptosis assay

To quantify the difference in cell death, the number of TUNEL-positive cells in the retina was counted in sagittal sections throughout the eye separated by intervals of 500 μm. At 7 days after light exposure, the TUNEL-positive cells appeared primarily in the INL and GCL of retina in MG rabbits (Fig. 4A). However, the number of apoptotic cells in both layers was significantly fewer in the retinas of C3G-, PCA-, and FA-treated rabbits than those in MG ($p < 0.05$; Fig. 4B).

3.4 HNE, 3-nitrotyrosine, and 8-OHdG levels in the retina

To evaluate oxidative stress status, the levels of HNE, 3-nitrotyrosine, and 8-OHdG in the retina were quantified by ELISA. After light exposure, HNE, 3-nitrotyrosine, and 8-OHdG levels were significantly increased in MG rabbits compared with those in NG ($p < 0.05$; Fig. 5A–C). However, the levels of HNE in C3G, PCA, and FA were significantly decreased than those in the MG ($p < 0.05$). The retinas of C3G and FA rabbits showed significant reduction in the levels of 3-nitrotyrosine and 8-OHdG compared with those in the MG ($p < 0.05$). The 3-nitrotyrosine and 8-OHdG levels were not significantly different between PCA and MG ($p > 0.05$).

3.5 Secretion and expression of HO-1 and Nrf2 in the retina

After light exposure, the HO-1 protein level was significantly increased as measured by Western blot analysis ($p < 0.05$; Figs. 6A and B). Treatment with C3G and FA significantly increased the expression of HO-1 compared with MG ($p < 0.05$). Furthermore, significant upregulation of HO-1 mRNA levels by C3G and FA treatments was confirmed by qPCR analysis ($p < 0.05$; Fig. 6C).

Light exposure induced a significant increase of the Nrf2 protein in the retina ($p < 0.05$; Fig. 7A). C3G, PCA, and FA treatments enhanced the light-induced increase in Nrf2 protein, although the difference with MG was not significant ($p > 0.05$). Consistent with its protein expression, the Nrf2 mRNA level was also increased by light exposure, although this increase was not statistically significant ($p > 0.05$; Fig. 7B). The Nrf2 mRNA levels were significantly increased in C3G and FA compared with MG ($p < 0.05$).

© 2016 WILEY-VCH Verlag GmbH & Co. KGaA, Weinheim

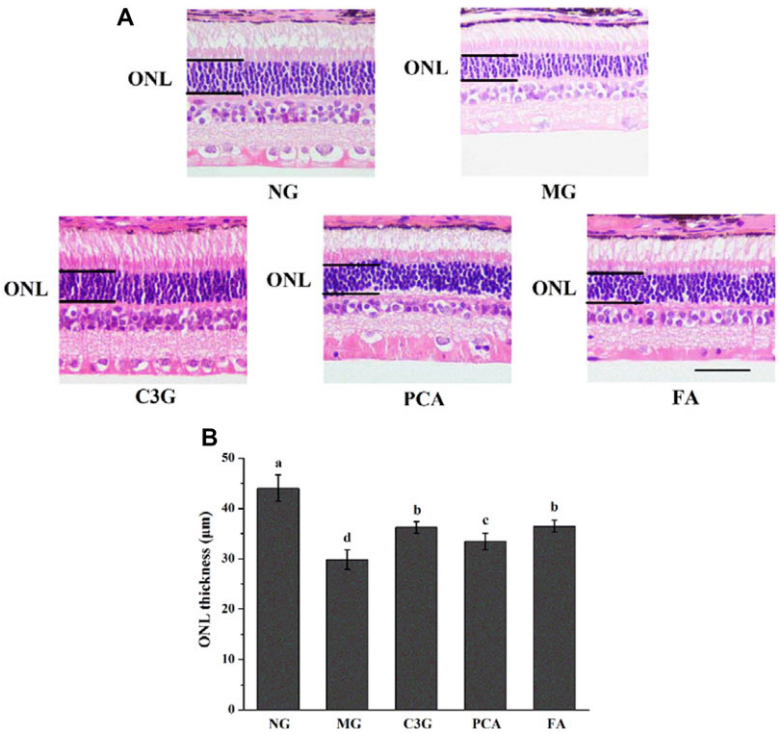

Figure 3. Effect of C3G, PCA, and FA on the retinal ONL thickness in rabbits at 7 days after light exposure. (A) Representative images of the HE-stained sections of rabbit retinas. Scale bar: 50 μm. (B) ONL thicknesses were measured within 250–2750 μm (counted at 500 μm intervals) of the superior and inferior edges from the ONH based on photographs of HE-stained sections by personnel blinded to the study groups. The mean ONL thickness was calculated from 12 sections for each retina. Data are expressed as mean ± standard deviation ($n = 8$). Bars not sharing a common capital letter are significantly different ($p < 0.05$) from each other, assayed by one-way ANOVA, followed by Duncan's multiple range test. ONL, outer nuclear layer; ONH, optic nerve head.

3.6 Secretion and expression of inflammatory related genes

Light exposure increased the secretion and expression of MCP-1, IL-8, and IL-1β (Fig. 8). Treatment with C3G, PCA, and FA significantly suppressed the photooxidation-induced increase in secretion of MCP-1 ($p < 0.05$; Fig. 8A). The data showed that treatment with FA significantly blocked the light-induced increase in IL-8 secretion ($p < 0.05$; Fig. 8C). C3G, PCA, and FA significantly reduced the increase in IL-8 mRNA

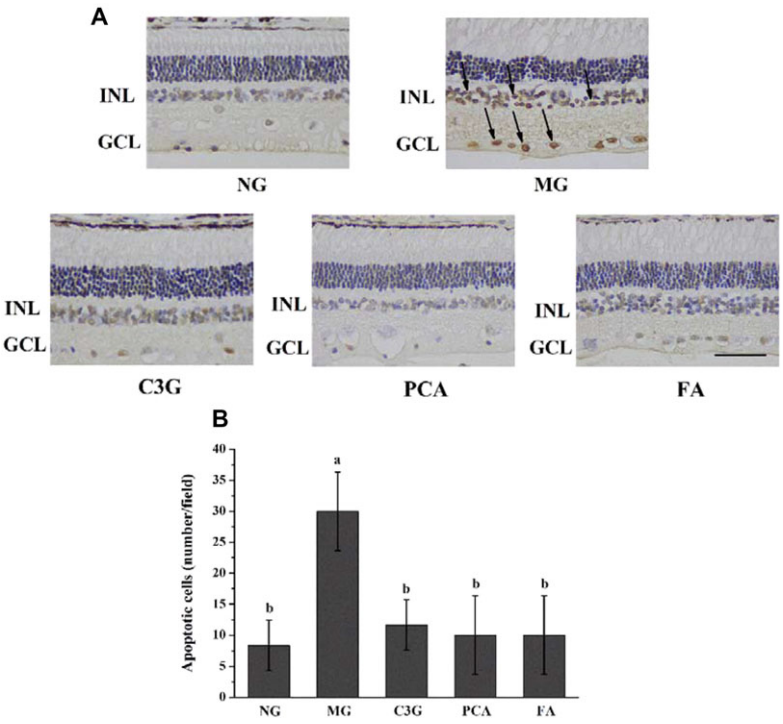

Figure 4. Effect of C3G, PCA, and FA treatments on the TUNEL staining of rabbit retinal sections at 7 days after light exposure. (A) Representative images of the TUNEL-stained sections of rabbit retinas. TUNEL-positive cells were present, with brown-stained nuclei. Scale bar: 50μm. (B) The number of TUNEL-positive cells was counted in ten sections per retina with an interval of 500 μm in the sagittal plane. Data are expressed as the mean ± standard deviation ($n = 8$). Bars not sharing a common capital letter are significantly different ($p < 0.05$) from each other, assayed by one-way ANOVA, followed by Duncan's multiple range test. INL, inner nuclear layer; GCL, ganglion cell layer.

© 2016 WILEY-VCH Verlag GmbH & Co. KGaA, Weinheim

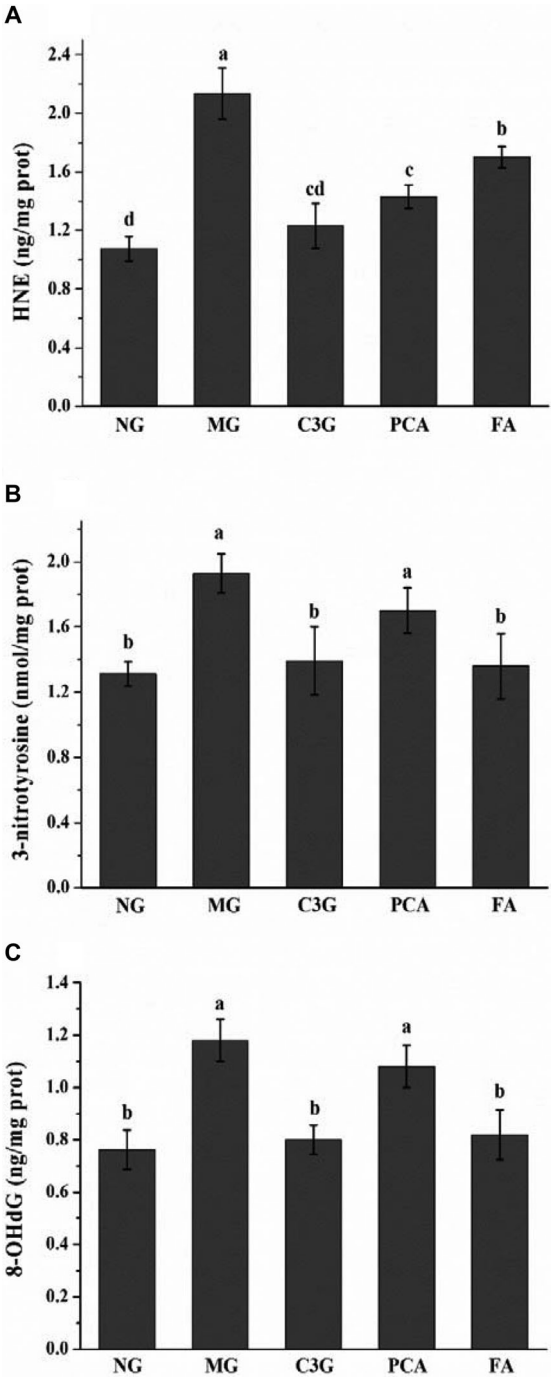

Figure 5. Effect of C3G, PCA, and FA treatments on the HNE, 3-nitrotyrosine, and 8-OHdG levels in the whole retina at 7 days after light exposure. Data are expressed as mean ± standard deviation ($n = 3$). Bars not sharing a common capital letter are significantly different ($p < 0.05$) from each other, assayed by one-way ANOVA, followed by Duncan's multiple range test. HNE: 4-hydroxynonenal; 8-OHdG: 8-hydroxydeoxyguanosine.

levels ($p < 0.05$; Fig. 8D). Treatment with C3G, PCA, and FA also significantly suppressed the photooxidation-induced increase in secretion and expression of IL-1β ($p < 0.05$; Figs. 8E and F).

After light exposure, markedly increased levels of TNF-α and nuclear factor kappa B (NF-κB) proteins were detected in the retina, whereas FA administration significantly reduced the TNF-α and NF-κB protein ($p < 0.05$; Figs. 9A, C, and D). COX-2 was also significantly elevated in the retina after light exposure ($p < 0.05$; Fig. 9B). However, the COX-2 levels in the retinas from C3G-, PCA-, and FA-treated rabbits were significantly lower than those in MG retinas ($p < 0.05$).

3.7 Expression of apoptosis-related proteins in the retina

The expression of apoptotic proteins was determined via immunohistochemistry or Western blot analysis. Caspase-3 activity was not detectable in the retina of NG rabbits (Fig. 10A). The expression of active caspase-3 was high in the INL and GCL of the rabbit retinas within the MG. However, treatment with C3G and its metabolites significantly reduced the upregulated expression of active caspase-3 in both layers ($p < 0.05$). The expression of active caspase-3 by immunohistochemistry was scored as shown in Fig. 10B. Light exposure significantly upregulated the pro-apoptotic protein active caspase-9 and Bax, but downregulated the anti-apoptotic protein Bcl-2 ($p < 0.05$; Figs. 10C–F). C3G and PCA significantly decreased level of expression of active caspase-9 protein ($p < 0.05$). C3G and its metabolites significantly increased the expression of Bcl-2 and decreased the expression of Bax ($p < 0.05$).

3.8 Secretion and expression of angiogenesis-related proteins in the retina

In this study, the effects of C3G and its metabolites on the vascular endothelial growth factor (VEGF) and HIF-1α expressions were investigated after light exposure. Light exposure significantly increased VEGF content in the retina of MG rabbits compared with those in NG ($p < 0.05$; Figs. 11A and B). By contrast, C3G and PCA treatment significantly decreased the level of VEGF in retina compared with those in MG ($p < 0.05$). In addition, the HIF-1α level in the retinas was significantly increased after light exposure, but its levels in the C3G-, PCA-, and FA-treated rabbits were significantly lower than those in MG retinas ($p < 0.05$; Fig. 11C).

4 Discussion

Berries are among the most widely consumed fruits in the human diet, and ACNs are known to be a major component of berries [24,25]. A recent human study showed that after the consumption of ACNs, the maximum concentration of PCA

© 2016 WILEY-VCH Verlag GmbH & Co. KGaA, Weinheim

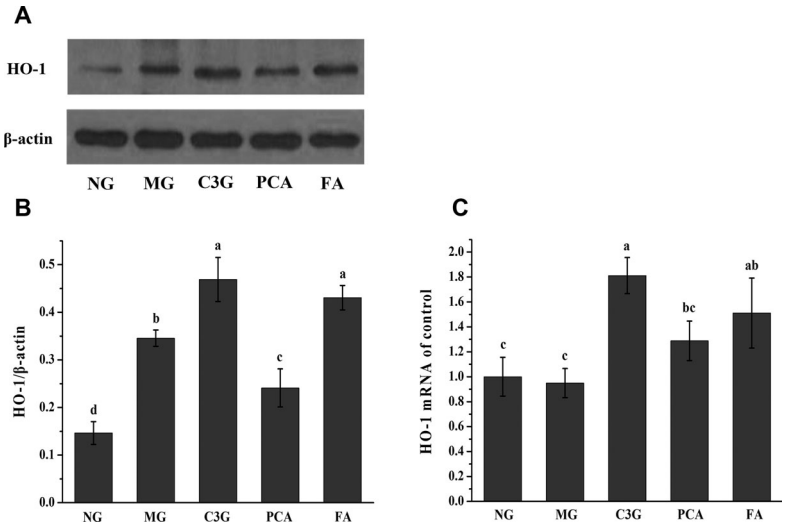

Figure 6. (A, C) Effect of C3G, PCA, and FA treatments on HO-1 (A) protein and (C) mRNA levels in the whole retina at 7 days after light exposure. (B) Densitometric analysis of HO-1 expression relative to the loading control (lower panel). Data are expressed as mean ± standard deviation ($n = 3$). Bars not sharing a common capital letter are significantly different ($p < 0.05$) from each other, assayed by one-way ANOVA, followed by Duncan's multiple range test. HO-1, heme oxygenase-1.

in the serum (approximately 492 nmol/L) is far higher than that of C3G (approximately 1.9 nmol/L) [15]. Another recent human study on the overall plasma bioavailability of C3G metabolites showed that PCA and FA absorbed in plasma could be detected at concentrations up to 2.35 and 0.94 μM for 48 h after consuming 500 mg of C3G, respectively [16]. Based on these findings, we hypothesized whether ACNs exerted their retinal protective effects at least partially through these important and major metabolites. However, most previous animal and in vitro studies have focused on the activity of the parent (un-metabolized) ACNs in models of retinal degeneration [12, 26]. Thus, the primary purpose of this study was to determine which metabolites that were produced after C3G consumption could play a major role in the beneficial effects on retinal degeneration in vivo.

C3G, PCA, and FA treatments protect the structure and function of photoreceptor cells from light-induced retinal degeneration. C3G and FA play a better role than PCA in reducing the levels of oxidative stress markers (3-nitrotyrosine and 8-OHdG) in the retina. C3G and FA also upregulated expression of Nrf2 transcription factors and phase II enzymes, such as HO-1, thereby suggesting that C3G and FA probably mediated the protection of retinal cells from light-induced damage by regulating the activation of the Nrf2/HO-1 pathway. C3G, PCA, and FA attenuated the photooxidation-induced changes in secretion and expression of inflammation-related genes (MCP-1, IL-8, and IL-1β). However, only FA suppressed NF-κB activation, which may underlie the mechanism of FA-mediated protection of retinal cells. Furthermore, C3G and its metabolites may play an important role in suppressing activation of the mitochondrial apoptotic pathways. In addition, C3G and PCA decreased the induction of VEGF and HIF-1α by light exposure in the retina. Results suggest that C3G and FA have better effects on reducing oxidative stress than PCA, whereas C3G and PCA have better effects on inhibiting angiogenesis than FA. All three treatments attenuated the photooxidation-induced inflammation and apoptosis.

The light damage reduces the b-wave amplitude of ERG and decreases the ONL thickness, which is consistent with previous reports [27]. Visual function was impaired in accordance with the photoreceptor cell loss (Fig. 3). However, treatment with C3G, PCA, and FA protects the structure and function of photoreceptor cells from light-induced damage. Furthermore, the protective effects of C3G and FA on the scotopic ERG and histological integrity of the retina were more pronounced than that of PCA, which possessed statistical significance ($p < 0.05$).

The mechanism of retinal light damage involves significant oxidative stress in pigmented rabbits has been established [21]. HNE, a mediator of cellular oxidative stress, is

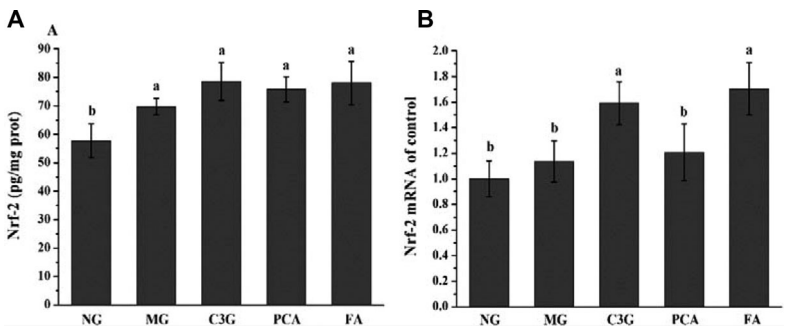

Figure 7. Effects of C3G, PCA, and FA treatments on Nrf2 (A) protein and (B) mRNA levels in the whole retina at 7 days after light exposure. Data are expressed as mean ± standard deviation ($n = 3$). Bars not sharing a common capital letter are significantly different ($p < 0.05$) from each other, assayed by one-way ANOVA, followed by Duncan's multiple range test. Nrf2, nuclear factor erythroid-2 related factor 2.

© 2016 WILEY-VCH Verlag GmbH & Co. KGaA, Weinheim

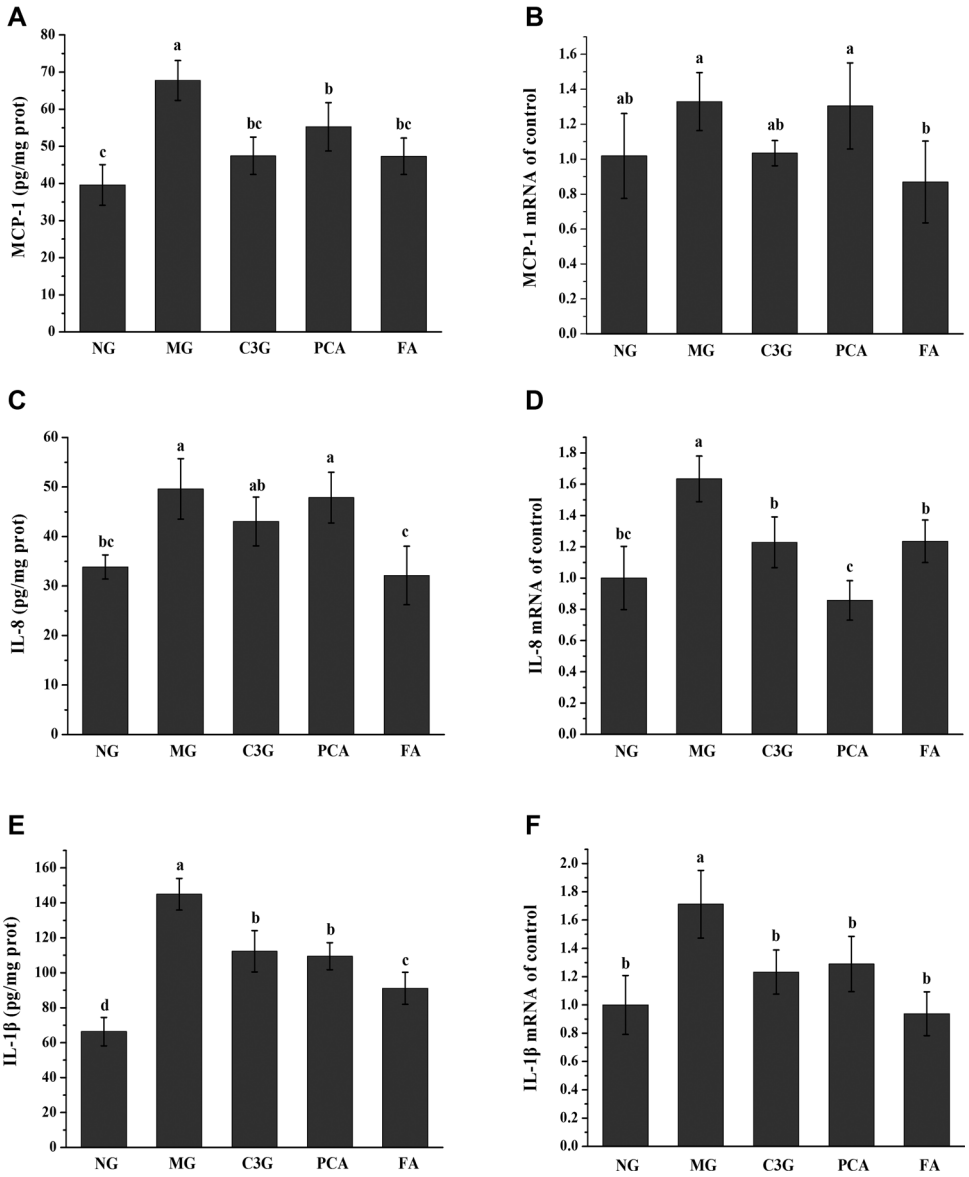

Figure 8. Effects of C3G, PCA, and FA treatments on (A, B) MCP-1, (C, D) IL-8, and (E, F) IL-1β (A, C, E) protein and (B, D, F) mRNA levels in the whole retina at 7 days after light exposure. Data are expressed as mean ± standard deviation ($n = 3$). Bars not sharing a common capital letter are significantly different ($p < 0.05$) from each other, assayed by one-way ANOVA, followed by Duncan's multiple range test. MCP-1, monocyte chemoattractant protein 1; IL-8, interleukine-8; IL-1β, interleukin-1 β.

generated by the nonenzymatic oxidation of n-6 PUFAs [28]. 3-Nitrotyrosine is another oxidative marker that is formed when tyrosine residues are attacked by peroxynitrite [29]. 8-OHdG is a product of oxidative DNA damage and a sensitive marker of increased oxidative stress [30]. Our data indicate that C3G and FA play a better role than PCA in reducing the levels of oxidative stress markers in the retina, which may be related to the underlying mechanism of C3G- and FA-mediated protection against photooxidation in the retina.

C3G and FA treatments simultaneously enhanced Nrf2 activation and increased HO-1 protein expression in the retina. Accumulating evidence suggests that HO-1 exerts potent endogenous anti-oxidative, anti-inflammatory, and anti-apoptotic properties [31]. As a stress inducible and redox-sensitive protein, HO-1 exerts potent indirect anti-oxidative functions by degrading heme to carbon monoxide, iron, and biliverdin [31]. Nrf2 is a transcription factor that regulates the expression of HO-1 [32]. These results suggest that C3G and FA are potent antioxidants for retinas. The protective effects of C3G and FA were mediated, at least in part, by the activation of the Nrf2/HO-1 antioxidant pathway in vivo.

In this retinal damage model, the expression of proinflammatory cytokines was increased (Figs. 8 and 9), which is consistent with previous reports that retinal oxidative stress activates NF-κB to upregulate the expression of proinflammatory cytokines (TNF-α, IL-1β, and MCP-1), chemokines (IL-8), and COX-2 [33, 34]. The evidence for the involvement of inflammation in AMD pathogenesis includes accumulation of immunoglobulin and complement components in

© 2016 WILEY-VCH Verlag GmbH & Co. KGaA, Weinheim

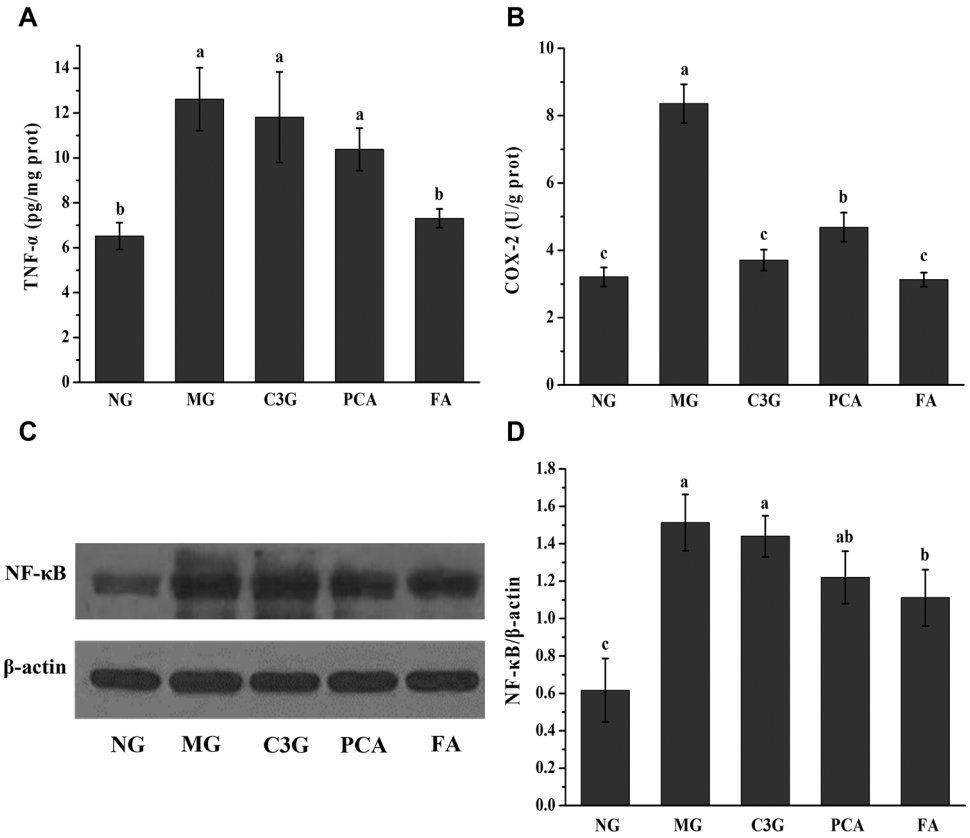

Figure 9. Effects of C3G, PCA, and FA treatments on (A) TNF-α, (B) COX-2, and (C) NF-κB protein levels in the entire retina at 7 days after light exposure. (D) Densitometric analysis of NF-κB expression relative to the loading control (lower panel). Data are expressed as mean ± standard deviation ($n = 3$). Bars not sharing a common letter are significantly different ($p < 0.05$) from each other, assayed by one-way ANOVA, followed by Duncan's multiple range test. TNF-α, tumor necrosis factor-alpha; COX-2, cyclooxygenase 2; NF-κB, nuclear factor kappa B.

drusen [35]. NF-κB is a key transcriptional regulator of several genes involved in oxidative stress and inflammatory responses [36, 37]. TNF-α upregulated the expression of various apoptotic factors and increased the secretion of VEGF in RPE cells in AMD [38, 39]. IL-1β is one of key mediators in intraocular inflammation that induce the expression of other cytokines and chemokines such as MCP-1 [40]. IL-8 is a neutrophil attractant and a strong proangiogenesis factor, which can promote inflammation and trigger neovascularization [41]. COX-2 leads to the synthesis of the proinflammatory prostaglandin E2 [42].

ACNs have been reported to inhibit the expression of TNF-α, IL-1β, MCP-1, and COX-2 [43–46], thereby exerting a significant anti-inflammatory effect. In a recent report, C3G and its metabolites altered the expression of inflammatory mediators in vitro; FA had the greatest effect on the reduction of the production of vascular cell adhesion molecule-1 protein [47]. When Min et al. [44] tested the anti-inflammatory effect of C3G and its metabolites, PCA exhibited better anti-inflammatory effect than C3G, but FA was not evaluated in their study. FA inhibited NF-κB activation in an in vitro model [48]. The present study provides clear evidence that FA administration alters the expression of related inflammatory genes and inhibits the activation of NF-κB in vivo. Furthermore, FA was more effective than PCA in suppressing the photooxidation-induced secretion of IL-8, IL-1β, TNF-α, and COX-2 in this study. These results suggest that the anti-inflammatory effects of ACNs are not limited to the parent structures themselves because their phenolic acids metabolites displayed even greater bioactivity. The reduced size and altered solubility of the metabolites could influence membrane penetration and increase access to intracellular mechanisms [49, 50]. In addition, previous studies indicated that ACNs inhibited proinflammatory cytokine production by regulating the activation of the NF-κB or mitogen-activated protein kinase (MAPK) pathway [51–53]. C3G inhibited proinflammatory cytokine production, possibly because it regulated the MAPK signaling pathway rather than inhibited the activation of NF-κB in this study.

Bcl-2 and Bax are key regulators of the mitochondrial pathways of apoptosis. No apoptotic photoreceptors are observed in retinas of Bax/Bak double knockout mice [54] and their apoptosis is effectively prevented by Bcl-2 overexpression [55]. In response to apoptotic stimuli, Bcl-2 family proteins mediated the activation of caspase-9, thereby triggering a cascade of caspase activation [56]. Visible light increased the retinal expression of Bax but decreased the Bcl-2 expression (Figs. 10C, E, and F). The data showed that treatment with C3G, PCA, and FA attenuated the light-induced increase in Bax expression and promoted Bcl-2 expression. Furthermore, light exposure led to a greater incidence of caspase-9 and caspase-3 cleavage in the retina; these events were attenuated by C3G, PCA, and FA. Thus, the consistent intake of C3G and its metabolites suppressed the activation of mitochondrial apoptotic

© 2016 WILEY-VCH Verlag GmbH & Co. KGaA, Weinheim

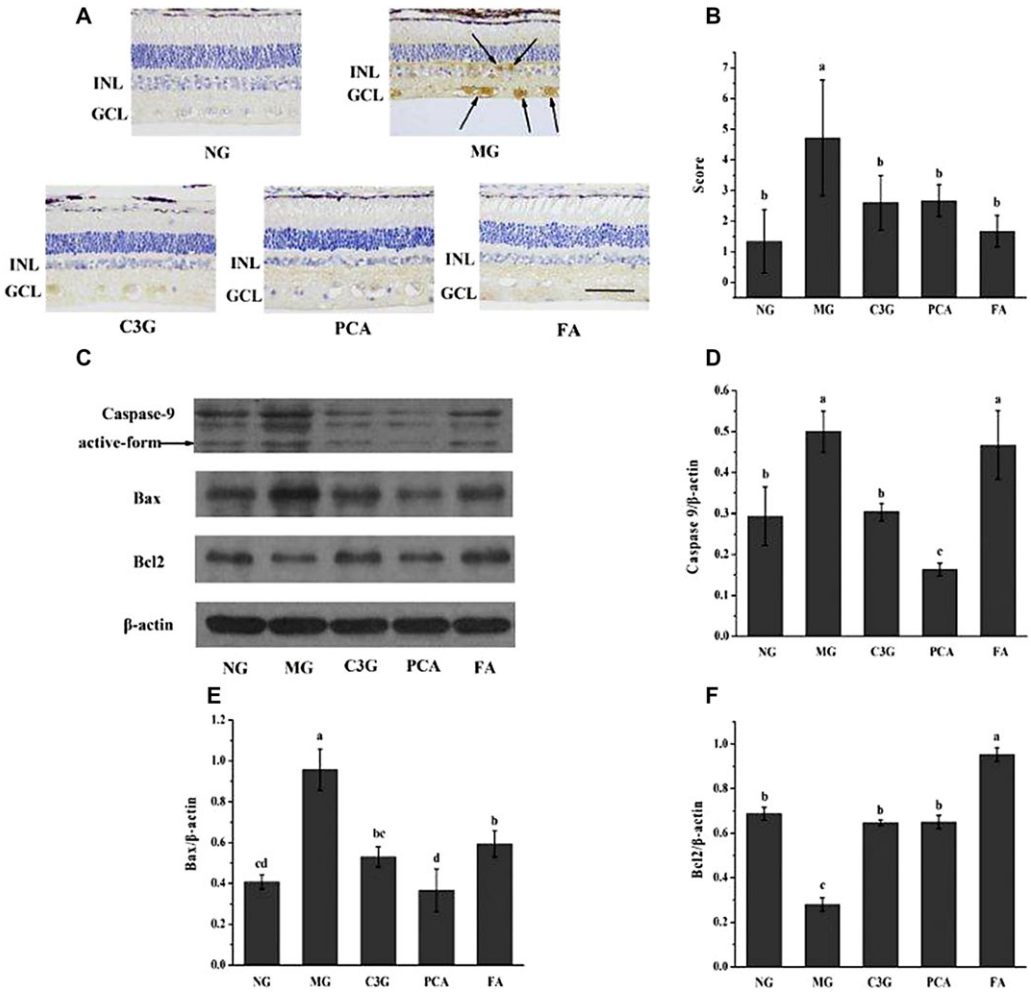

Figure 10. (A, C) Effects of C3G, PCA, and FA treatments on (A) active caspase-3 expression in the retina and (C) caspase-9, Bax, and Bcl-2 protein expression in the whole retina at 7 days after light exposure. Active caspase-3 cells were present, with brown-stained nuclei. Scale bar: 50 μm. (B) Scores were determined by evaluating the extent and intensity of immunopositivity. (D–F) Densitometric analysis of (D) caspase-9, (E) Bax, and (F) Bcl-2 expressions relative to the loading control (lower panel). Data are expressed as mean ± standard deviation ($n = 3$). Bars not sharing a common letter are significantly different ($p < 0.05$) from each other, assayed by one-way ANOVA, followed by Duncan's multiple range test. INL, inner nuclear layer; GCL, ganglion cell layer.

pathways and eventually attenuated the extent of light-induced apoptosis of retinal cells.

ACNs may act to prevent angiogenesis, such that the ACN-rich extract alleviated the induction of VEGF and HIF-1α in vivo and in vitro [57]. Similar anti-angiogenic effects of ACN-rich extracts have been reported by other authors [58, 59]. Proangiogenic cytokines have been shown to be involved in the onset and/or development of AMD, with VEGF playing the most important role of neovascularizaton and increasing permeability [60]. HIF-1α is the major hypoxia sensor and plays a central role in controlling the expression of genes involved in angiogenesis [61]. Our findings are in agreement with this previous work and provide additional evidence that C3G and its metabolites suppress angiogenesis.

The present study provides novel insights into the retinal protective activity of C3G and its metabolites but this experimental approach has several limitations. The most important potential limitation of our experimental study is that we chose a dose of C3G, PCA, and FA, which may represent reasonable dietary intake; all treatments are given via gavage at the same concentration. This approach may not reflect the different dietary abundance of these compounds or the different bioavailability among the compounds. Future studies are required to explore a greater range of physiologically appropriate concentrations for these compounds. In addition, future studies need to investigate whether C3G inhibited proinflammatory cytokine production by regulating the MAPK signaling pathway at the same dose in this study.

To the best of our knowledge, this work is the first in vivo study to demonstrate that C3G and its metabolites possess a combination of retinal protective effects, including the

© 2016 WILEY-VCH Verlag GmbH & Co. KGaA, Weinheim

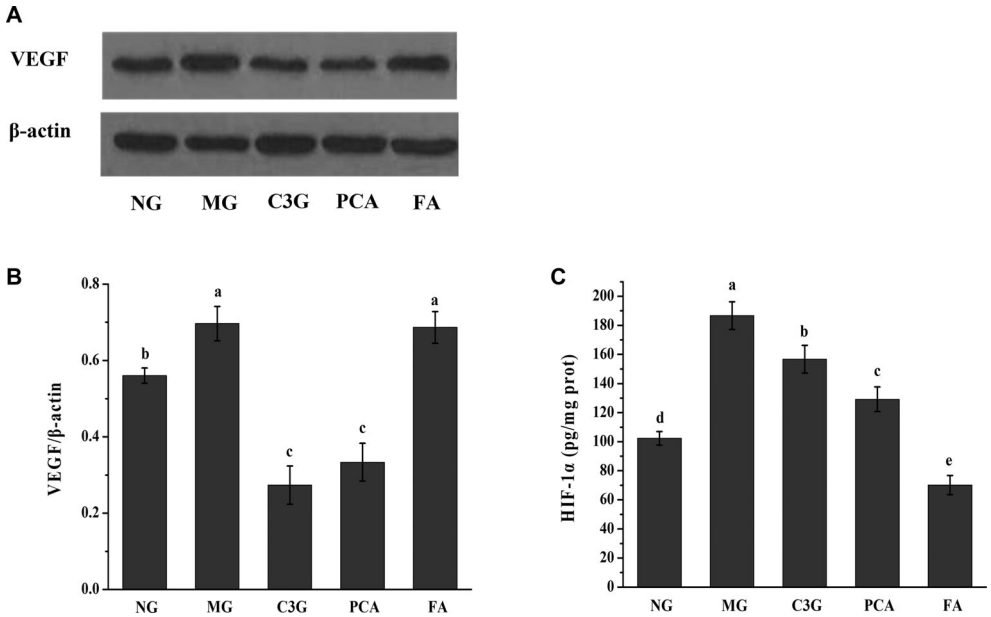

Figure 11. (A) Effects of C3G, PCA, and FA treatments on VEGF protein levels in the whole retina at 7 days after light exposure. (B) Densitometric analysis of VEGF expression relative to the loading control (lower panel). (C) Effects of C3G, PCA, and FA treatments on HIF-1α protein levels in the whole retina at 7 days after light exposure. Data are expressed as mean ± standard deviation ($n = 3$). Bars not sharing a common capital letter are significantly different ($p < 0.05$) from each other, assayed by one-way ANOVA, followed by Duncan's multiple range test. VEGF, vascular endothelial growth factor; HIF-1α, hypoxia-inducible factor-1α.

activation of Nrf2/HO-1 pathway, the inhibition of NF-κB activation, and the anti-angiogenesis against visible light-induced retinal degeneration. The roles of C3G and its metabolites in modulating oxidative stress and inflammation-related genes may be the mechanisms by which dietary C3G can reduce the risk of AMD. This finding also suggests that the metabolism of ACNs, such as PCA and FA, does not reduce their bioactivity and may enhance it in some instances.

This work was financially supported by the National Natural Science Foundation of China (No. 31571831).

Y.W. and B.J. conceived and designed the experiments. Y.W., Y.H., L.Z., F.L., O.W., and X.Y. performed the experiments. Y.W. and F.Z. analyzed the data. F.Z. contributed reagents/materials/analysis tools. Y.W. wrote the paper.

The authors have declared no conflict of interest.

5 References

[1] Hunter, J. J., Morgan, J. I. W., Merigan, W. H., Sliney, D. H. et al., The susceptibility of the retina to photochemical damage from visible light. *Prog. Retin. Eye Res.* 2012, *31*, 28–42.

[2] Wenzel, A., Grimm, C., Samardzija, M., Reme, C. E., Molecular mechanisms of light-induced photoreceptor apoptosis and neuroprotection for retinal degeneration. *Prog. Retin. Eye Res.* 2005, *24*, 275–306.

[3] Wu, J., Seregard, S., Algvere, P. V., Photochemical damage of the retina. *Surv. Ophthalmol.* 2006, *51*, 461–481.

[4] Jarrett, S. G., Boulton, M. E., Consequences of oxidative stress in age-related macular degeneration. *Mol. Aspects Med.* 2012, *33*, 399–417.

[5] Zafra-Stone, S., Yasmin, T., Bagchi, M., Chatterjee, A. et al., Berry anthocyanins as novel antioxidants in human health and disease prevention. *Mol. Nutr. Food Res.* 2007, *51*, 675–683.

[6] Matsunaga, N., Imai, S., Inokuchi, Y., Shimazawa, M. et al., Bilberry and its main constituents have neuroprotective effects against retinal neuronal damage in vitro and in vivo. *Mol. Nutr. Food Res.* 2009, *53*, 869–877.

[7] Tremblay, F., Waterhouse, J., Nason, J., Kalt, W., Prophylactic neuroprotection by blueberry-enriched diet in a rat model of light-induced retinopathy. *J. Nutr. Biochem.* 2013, *24*, 647–655.

[8] Harborne, J. B., Williams, C. A., Anthocyanins and other flavonoids. *Nat. Prod. Rep.* 2001, *18*, 310–333.

[9] Matsumoto, H., Nakamura, Y., Tachibanaki, S., Kawamura, S. et al., Stimulatory effect of cyanidin 3-glycosides on the regeneration of rhodopsin. *J. Agr. Food Chem.* 2003, *51*, 3560–3563.

[10] Wang, Y., Zhang, D., Liu, Y., Wang, D. et al., The protective effects of berry-derived anthocyanins against visible light-induced damage in human retinal pigment epithelial cells. *J. Sci. Food Agr.* 2015, *95*, 936–944.

[11] Tirupula, K. C., Balem, F., Yanamala, N., Klein-Seetharaman, J., pH-dependent Interaction of Rhodopsin with Cyanidin-

© 2016 WILEY-VCH Verlag GmbH & Co. KGaA, Weinheim

3-glucoside. *2. Functional Aspects. Photochem. Photobiol.* 2009, *85*, 463–470.

[12] Jang, Y. P., Zhou, J. L., Nakanishi, K., Sparrow, J. R., Anthocyanins protect against A2E photooxidation and membrane permeabilization in retinal pigment epithelial cells. *Photochem. Photobiol.* 2005, *81*, 529–536.

[13] Sun, M., Lu, X., Hao, L., Wu, T. et al., The influences of purple sweet potato anthocyanin on the growth characteristics of human retinal pigment epithelial cells. *Food Nutr. Res.* 2015, *59*, 27830.

[14] Kalt, W., Blumberg, J. B., McDonald, J. E., Vinqvist-Tymchuk, M. R. et al., Identification of anthocyanins in the liver, eye, and brain of blueberry-fed pigs. *J. Agr. Food Chem.* 2008, *56*, 705–712.

[15] Vitaglione, P., Donnarumma, G., Napolitano, A., Galvano, F. et al., Protocatechuic acid is the major human metabolite of cyanidin-glucosides. *J. Nutr.* 2007, *137*, 2043–2048.

[16] Czank, C., Cassidy, A., Zhang, Q., Morrison, D. J. et al., Human metabolism and elimination of the anthocyanin, cyanidin-3-glucoside: a C-13-tracer study. *Am. J. Clin. Nutr.* 2013, *97*, 995–1003.

[17] Kassoff, A., Kassoff, J., Buehler, J., Eglow, M. et al., A randomized, placebo-controlled, clinical trial of high-dose supplementation with vitamins C and E, beta carotene, and zinc for age-related macular degeneration and vision loss - AREDS Report No. *8. Arch. Ophthalmol.* 2001, *119*, 1417–1436.

[18] Jang, H., Ahn, H. R., Jo, H., Kim, K. A. et al., Chlorogenic acid and coffee prevent hypoxia-induced retinal degeneration. *J. Agr. Food Chem.* 2014, *62*, 182–191.

[19] Ahn, H. R., Lee, H. J., Kim, K. A., Kim, C. Y. et al., Hydroxycinnamic acids in crepidiastrum denticulatum protect oxidative stress-induced retinal damage. *J. Agr. Food Chem.* 2014, *62*, 1310–1323.

[20] Larrosa, M., Lodovici, M., Morbidelli, L., Dolara, P., Hydrocaffeic and p-coumaric acids, natural phenolic compounds, inhibit UV-B damage in WKD human conjunctival cells in vitro and rabbit eye in vivo. *Free Radical Res.* 2008, *42*, 903–910.

[21] Wang, Y., Zhao, L., Lu, F., Yang, X. et al., Retinoprotective effects of bilberry anthocyanins via antioxidant, anti-inflammatory, and anti-apoptotic mechanisms in a visible light-induced retinal degeneration model in pigmented rabbits. *Molecules* 2015, *20*, 22395–22410.

[22] Wang, Y., Huang, FH., Zhao, L., Zhang, D. et al., Protective effect of total flavones from hippophae rhamnoides l. against visible light-induced retinal degeneration in pigmented rabbits. *J. Agric. Food Chem.* 2016, *64*, 161–170.

[23] Livak, K. J., Schmittgen, T. D., Analysis of relative gene expression data using real-time quantitative PCR and the 2(T)(-Delta Delta C) method. *Methods* 2001, *25*, 402–408.

[24] Banaszewski, K., Park, E. Y., Edirisinghe, I., Cappozzo, J. C. et al., A pilot study to investigate bioavailability of strawberry anthocyanins and characterize postprandial plasma polyphenols absorption patterns by Q-TOF LC/MS in humans. *J. Berry Res.* 2013, *3*, 113–126.

[25] Giampieri, F., Alvarez-Suarez, J. M., Tulipani, S., Gonzales-Paramas, A. M. et al., Photoprotective Potential of Strawberry (Fragaria x ananassa) Extract against UV-A Irradiation Damage on Human Fibroblasts. *J. Agric. Food Chem.* 2012, *60*, 2322–2327.

[26] Miyake, S., Takahashi, N., Sasaki, M., Kobayashi, S. et al., Vision preservation during retinal inflammation by anthocyanin-rich bilberry extract: cellular and molecular mechanism. *Lab. Invest.* 2012, *92*, 102–109.

[27] Sasaki, M., Yuki, K., Kurihara, T., Miyake, S. et al., Biological role of lutein in the light-induced retinal degeneration. *J. Nutr. Biochem.* 2012, *23*, 423–429.

[28] Catala, A., Lipid peroxidation of membrane phospholipids generates hydroxy-alkenals and oxidized phospholipids active in physiological and/or pathological conditions. *Chem. Phys. Lipids* 2009, *157*, 1–11.

[29] Song, D., Song, Y., Hadziahmetovic, M., Zhong, Y. et al., Systemic administration of the iron chelator deferiprone protects against light-induced photoreceptor degeneration in the mouse retina. *Free Radical Bio. Med.* 2012, *53*, 64–71.

[30] Liu, Y., Tang, L. S., Chen, B. H., Effects of antioxidant gene therapy on retinal neurons and oxidative stress in a model of retinal ischemia/reperfusion. *Free Radical Bio. Med.* 2012, *52*, 909–915.

[31] Fan, J., Xu, G., Jiang, T., Qin, Y., Pharmacologic induction of heme oxygenase-1 plays a protective role in diabetic retinopathy in rats. *Invest. Ophth. Vis. Sci.* 2012, *53*, 6541–6556.

[32] Itoh, K., Wakabayashi, N., Katoh, Y., Ishii, T. et al., Keap1 represses nuclear activation of antioxidant responsive elements by Nrf2 through binding to the amino-terminal Neh2 domain. *Gene. Dev.* 1999, *13*, 76–86.

[33] Hoesel, B., Schmid, J. A., The complexity of NF-kappa B signaling in inflammation and cancer. *Mol. Cancer.* 2013, *12*, 1–15.

[34] Kaarniranta, K., Salminen, A., NF-kappa B signaling as a putative target for omega-3 metabolites in the prevention of age-related macular degeneration (AMD). *Exp. Gerontol.* 2009, *44*, 685–688.

[35] Bian, Q., Gao, S., Zhou, J., Qin, J. et al., Lutein and zeaxanthin supplementation reduces photooxidative damage and modulates the expression of inflammation-related genes in retinal pigment epithelial cells. *Free Radical Bio. Med.* 2012, *53*, 1298–1307.

[36] Mandal, M. N. A., Patlolla, J. M. R., Zheng, L., Agbaga, M. P. et al., Curcumin protects retinal cells from light-and oxidant stress-induced cell death. *Free Radical Bio. Med.* 2009, *46*, 672–679.

[37] Lee, Y. H., Kumar, N. C., Glickman, R. D., Modulation of photochemical damage in normal and malignant cells by naturally occurring compounds. *Photochem. Photobiol.* 2012, *88*, 1385–1395.

[38] Yang, P., McKay, B. S., Allen, J. B., Jaffe, G. J., Effect of NF-kappa B inhibition on TNF-alpha-induced apoptosis in human RPE cells. *Invest. Ophth. Vis. Sci.* 2004, *45*, 2438–2446.

[39] Nagineni, C. N., Kommineni, V. K., William, A., Detrick, B. et al., Regulation of VEGF expression in human retinal cells

© 2016 WILEY-VCH Verlag GmbH & Co. KGaA, Weinheim

by cytokines: implications for the role of inflammation in age-related macular degeneration. *J. Cell. Physiol.* 2012, *227*, 116–126.

[40] Bian, Z. M., Elner, S. G., Yoshida, A., Kunkel, S. L. et al., Activation of p38, ERK1/2 and NIK pathways is required for IL-1 beta and TNF-alpha-induced chemokine expression in human retinal pigment epithelial cells. *Exp. Eye Res.* 2001, *73*, 111–121.

[41] Simonini, A., Moscucci, M., Muller, D. W. M., Bates, E. R. et al., IL-8 is an angiogenic factor in human coronary atherectomy tissue. *Circulation* 2000, *101*, 1519–1526.

[42] Chen, A. C., Damian, D. L., Halliday, G. M., Oral and systemic photoprotection. *Photodermatol. Photo.* 2014, *30*, 102–111.

[43] Li, J., Lim, S. S., Lee, J. Y., Kim J-K. et al., Purple corn anthocyanins dampened high-glucose-induced mesangial fibrosis and inflammation: possible renoprotective role in diabetic nephropathy. *J. Nutr. Biochem.* 2012, *23*, 320–331.

[44] Min, S. W., Ryu, S. N., Kim, D. H., Anti-inflammatory effects of black rice, cyanidin-3-O-beta-D-glycoside, and its metabolites, cyanidin and protocatechuic acid. *Int. Immunopharmacol.* 2010, *10*, 959–966.

[45] Joseph, S. V., Edirisinghe, I., Burton-Freeman, B. M., Berries: anti-inflammatory effects in humans. *J. Agric. Food Chem.* 2014, *62*, 3886–3903.

[46] Giampieri, F., Forbes-Hernandez, T. Y., Gasparrini, M., Alvarez-Suarez, J. M. et al., Strawberry as a health promoter: an evidence based review. *Food Funct.* 2015, *6*, 1386–1398.

[47] Amin, H.P., Czank, C., Raheem, S., Zhang, Q. et al., Anthocyanins and their physiologically relevant metabolites alter the expression of IL-6 and VCAM-1 in CD40L and oxidized LDL challenged vascular endothelial cells. *Mol. Nutr. Food Res.* 2015, *59*, 1095–1106.

[48] Ma, Z. C., Hong, Q., Wang, Y. G., Tan, H. L. et al., Ferulic acid attenuates adhesion molecule expression in gamma-radiated human umbilical vascular endothelial cells. *Biol. Pharm. Bull.* 2010, *33*, 752–58.

[49] Gao, S., Hu, M., Bioavailability challenges associated with development of anti-cancer phenolics. *Mini-Rev. Med. Chem.* 2010, *10*, 550–567.

[50] Passamonti, S., Terdoslavich, M., Franca, R., Vanzo, A. et al., Bioavailability of flavonoids: a review of their membrane transport and the function of bilitranslocase in animal and plant organisms. *Curr. Drug Metab.* 2009, *10*, 369–394.

[51] Speciale, A., Canali, R., Chirafisi, J., Saija, A. et al., Cyanidin-3-O-glucoside protection against TNF-alpha-induced endothelial dysfunction: involvement of nuclear factor-kappa B signaling. *J. Agric. Food Chem.* 2010, *58*, 12048–12054.

[52] Lee, S. G., Kim, B., Yang, Y., Pham, T. X. et al., Berry anthocyanins suppress the expression and secretion of proinflammatory mediators in macrophages by inhibiting nuclear translocation of NF-kappa B independent of NRF2-mediated mechanism. *J. Nutr. Biochem.* 2014, *25*, 404–411.

[53] Afaq, F., Malik, A., Syed, D., Maes, D. et al., Pomegranate fruit extract modulates UV-B-mediated phosphorylation of mitogen-activated protein kinases and activation of nuclear factor kappa B in normal human epidermal keratinocytes. *Photochem. Photobiol.* 2005, *81*, 38–45.

[54] Hahn, P., Lindsten, T., Ying, G. S., Bennett, J. et al., Proapoptotic Bcl-2 family members, Bax and Bak, are essential for developmental photoreceptor apoptosis. *Invest. Ophth. Vis. Sci.* 2003, *44*, 3598–3605.

[55] Strettoi, E., Volpini, M., Retinal organization in the bcl-2-overexpressing transgenic mouse. *J. Comp. Neurol.* 2002, *446*, 1–10.

[56] Park, H. S., Han, M. H., Kim, G. Y., Moon, S. K. et al., Sulforaphane induces reactive oxygen species-mediated mitotic arrest and subsequent apoptosis in human bladder cancer 5637 cells. *Food Chem. Toxicol.* 2014, *64*, 157–165.

[57] Kang, M. K., Lim, S. S., Lee, J. Y., Yeo, K. M. et al., Anthocyanin-rich purple corn extract inhibit diabetes-associated glomerular angiogenesis. *Plos One* 2013, *8*, e79823.

[58] Matsubara, K., Kaneyuki, T., Miyake, T., Mori, M., Antiangiogenic activity of nasunin, an antioxidant anthocyanin, in eggplant peels. *J. Agr. Food Chem.* 2005, *53*, 6272–6275.

[59] Matsunaga, N., Tsuruma, K., Shimazawa, M., Yokota, S. et al., Inhibitory actions of bilberry anthocyanidins on angiogenesis. *Phytother. Res.* 2010, *24*, S42–S47.

[60] Witmer, A. N., Vrensen, G., Van Noorden, C. J. F., Schlingemann, R. O., Vascular endothelial growth factors and angiogenesis in eye disease. *Prog. Retinal Eye Res.* 2003, *22*, 1–29.

[61] Pistollato, F., Bremer-Hoffmann, S., Basso, G., Cano, S. S. et al. Targeting glioblastoma with the use of phytocompounds and nanoparticles. *Target. Oncol.* 2015, *11*, 1–16.

© 2016 WILEY-VCH Verlag GmbH & Co. KGaA, Weinheim